Midterm Technical Report No. 4B *May 1976*
Covering the Period August 8, 1975 to April 15, 1976
SRI No. MP 75-47

NEW ELECTRONIC-TRANSITION LASER SYSTEMS

Part II: Chemically Pumped Systems

By: D. J. ECKSTROM, S. G. PRAKASH, B. E. PERRY,
and S. W. BENSON

Prepared for:

DEFENSE ADVANCED RESEARCH PROJECTS AGENCY
WASHINGTON, D. C. 20301
AND
U. S. ARMY MISSILE COMMAND
REDSTONE ARSENAL, ALABAMA 35809

ARPA Order No. 1180
Contract DAAH01-74-C-0524 (8 February 1974 to 15 August 1976)
Contract Amount $763,482

SRI Project PYU-3190

STANFORD RESEARCH INSTITUTE
Menlo Park, California 94025 · U.S.A.

MISSING PAGE
NUMBERS ARE BLANK
AND WERE NOT
FILMED

Unclassified

SECURITY CLASSIFICATION OF THIS PAGE (When Data Entered)

REPORT DOCUMENTATION PAGE

READ INSTRUCTIONS BEFORE COMPLETING FORM

1. REPORT NUMBER

2. GOVT ACCESSION NO.

3. RECIPIENT'S CATALOG NUMBER

4. TITLE (and Subtitle)
New Electronic-Transition Laser Systems. Part II. Chemically Pumped Systems.

5. TYPE OF REPORT & PERIOD COVERED
Midterm Technical No. 4B
(8/8/75-5/15/76)

6. PERFORMING ORG. REPORT NUMBER
SRI - MP-76-47

7. AUTHOR(s)
D. J. Eckstrom, S. G. Prakash, B. E. Perry, and S. W. Benson

8. CONTRACT OR GRANT NUMBER(s)
DAAH01-74-C-0524, ARPA Order-1180

9. PERFORMING ORGANIZATION NAME AND ADDRESS
Stanford Research Institute
333 Ravenswood Avenue
Menlo Park, California 94025

10. PROGRAM ELEMENT, PROJECT, TASK AREA & WORK UNIT NUMBERS

11. CONTROLLING OFFICE NAME AND ADDRESS
Defense Advanced Research Projects Agency
1400 Wilson Boulevard
Arlington, Virginia 22209

12. REPORT DATE
May 1976

13. NO. OF PAGES
50

14. MONITORING AGENCY NAME & ADDRESS (If diff. from Controlling Office)
U.S. Army Missile Command
Redstone Arsenal, Alabama 35809

15. SECURITY CLASS. (of this report)
Unclassified

15a. DECLASSIFICATION/DOWNGRADING SCHEDULE

16. DISTRIBUTION STATEMENT (of this report)
Distribution of this document is unlimited.

SRI-PYU-3190

17. DISTRIBUTION STATEMENT (of the abstract entered in Block 20, if different from report)

18. SUPPLEMENTARY NOTES
Midterm technical rept. no. 4B
8 Aug 75 - 15 Apr 76

19. KEY WORDS (Continue on reverse side if necessary and identify by block number)
visible chemical lasers, chemiluminescence, metal atom combustion, photon yields

20. ABSTRACT (Continue on reverse side if necessary and identify by block number)
We report experimental and analytical studies aimed at development of visible chemical lasers. During this period, intracavity dye laser measurements of a Ba + N_2O flame revealed absorption on several BaO transitions and indicated large concentrations of Ba and $Ba^{(+)}$ metastables. Additional measurements on Ba + N_2O in a heat-pipe-oven reactor confirmed the dominant role of metal atom density on BaO photon yield, and showed that current kinetic models are inadequate. Imposition of microwave and dc electric fields on a Ba + N_2O flame decreased

CONTINUED

DD FORM 1 JAN 73 1473
EDITION OF 1 NOV 65 IS OBSOLETE

Unclassified

SECURITY CLASSIFICATION OF THIS PAGE (When Data Entered)

332500

20 ABSTRACT (Continued)
BaO emission, thus reducing hopes for a hybrid discharge-chemical laser.

A shock tube program was initiated to study premixed, pulsed reactions of volatile encapsulated metals with oxidizers. So far, we have examined $Ni(CO)_4$ with N_2O and NF_3 and $Sn(CH_3)_4$ with N_2O. Molecular emission from these reactions was much weaker than anticipated. In particular, we observed only SnO(D-X) bands rather than the a-X and A-X bands expected on the basis of flame studies.

An analysis of the excited molecular state production expected from atom association reactions in a shock tube-expansion nozzle environment indicates that the maximum gain expected is less than 10^{-6}/cm. Thus, this does not appear to be a feasible approach to development of visible chemical lasers.

10 TO THE MINUS 6TH POWER PER CM.

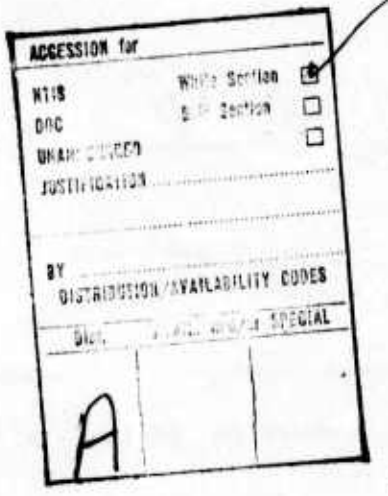

CONTENTS

SUMMARY

We report here experimental and analytical results from an ongoing program aimed at the development of visible chemical lasers. This study has concentrated on the highly exothermic reactions of metal atoms with various oxidizers.

During this period, we used intracavity dye laser measurements to establish the existence of absorption rather than gain on several bands in the BaO($A^1\Sigma$-$X^1\Sigma$) system. These measurements also verified the presence of large concentrations of Ba metastables in the flame and demonstrated for the first time the presence of large concentrations of Ba^+ ions. These experiments will be continued.

Additional measurements were made on Ba + N_2O in a heat-pipe-oven reactor. We found increasing evidence for the dominant effect of Ba concentration on BaO photon yields and concluded that previously formulated kinetic models do not adequately explain the results.

Emission from the Ba + N_2O reaction in the presence of microwave and glow discharge electric fields was studied with a view towards the prospect of a hybrid discharge-chemical laser. Contrary to our expectations, the BaO emission decreased when strong fields were applied.

During this period, we initiated a shock tube study of premixed, pulsed reactions that was aimed at achieving high reaction rates without the deleterious effects of reactant quenching and vibrational relaxation. So far we have studied reactions of $Ni(CO)_4$ with N_2O and NF_3 and of $Sn(CH_3)_4$ with N_2O. No NiO emission was observed, and NiF emission is considered to be thermal in origin. We have observed moderate amounts of SnO(D-X) emission but none of the anticipated SnO(a-X) systems. These studies are continuing.

We also analyzed the feasibility of achieving a visible chemical laser by atom association reactions in a shock tube expansion nozzle environment. We must confine our considerations to the few reactions for which sufficient data exist, but we predict very low gains at best for those cases. We conclude that this is not a promising approach, in accord with negative experimental results in other laboratories.

ILLUSTRATIONS

TABLES

INTRODUCTION

The objective of this research is to develop an electronic transition (visible or near visible) chemical laser. The premise of the work is that observation of visible chemiluminescence in flames indicates the existence of binary reactions,

$$A + BC \rightarrow AB^{*} + C$$

$$\rightarrow AB + C^{*} ,$$

which can lead to electronic excitation and subsequent radiation. We have sought exothermic reactions, primarily of metal atoms, that produce sufficient excited-state populations, and, in fact, population inversion, of either molecules or atoms, to produce laser action. We have found several that do have high photon yields, but the existence of population inversions has yet to be established. In addition, the kinetic processes leading to radiation are not yet well understood, and the feasibility of scaling reaction rates to laser conditions has not been determined.

During this reporting period, we have initiated three experimental programs and continued a fourth in search of understanding of these problems. These studies and their specific goals are:

(1) Intracavity dye laser gain/absorption measurements were made by a very sensitive technique in an attempt to establish whether gain or absorption exists on molecular transitions in Ba + N_2O.

(2) Heat-pipe-oven reactor studies of the Ba + N_2O reaction were continued to study metal atom quenching and reaction kinetics.

(3) Effects of electric fields on Ba + N_2O flames were studied to examine the possibility of enhancing emission from flames in order to develop a hybrid electrical-chemical laser.

(4) Shock tube studies of premixed, pulsed reactions were initiated in an attempt to obtain high reaction rates per unit volume by using premixed, volatile reactants, and to overcome problems of reactant quenching and vibrational relaxation by making the reaction rapid.

In addition to these experimental studies, we analyzed the feasibility of generating visible chemical laser action through atom association reactions. This was probably the first scheme proposed for electronic-transition chemical lasers. We considered the conditions pertinent to shock tube/expansion nozzle environments.

INTRACAVITY DYE LASER ABSORPTION/GAIN MEASUREMENTS

The dye laser, spectroscopic, and analytical aspects of these experiments were carried out by Mr. James P. Reilly, Department of Chemistry, University of California at Berkeley; we express our appreciation to him.

Background

One approach to the development of new laser systems is to carry out sufficient kinetic studies so that the populations of upper and lower laser levels can be calculated and the existence of gain predicted. A less informative, but still useful, alternative is to make direct gain and/or absorption measurements at appropriate wavelengths for the candidate systems at a variety of conditions in the range considered optimum. In the past, we have searched for gain in the Ba + N_2O and Sm + NF_3 systems by resonant cavity spectroscopy,[1] with no evidence for gain observed. During this period, we collaborated with Dr. M. Steinberg of the University of California at Santa Barbara, who repeated the measurements for Ba + N_2O. Again, there was no evidence of gain on BaO transitions. There was some evidence for enhancement of the Ba 7120 Å line [$6p'\,^1D_2^o$-$5d^3D_1$], but the effect was not repeatable.

In an attempt to obtain a more sensitive, and thus more definitive measurement of gain/absorption on candidate chemical laser reactions, we instituted a series of intracavity dye laser measurements.[2] This technique has been reported to be sensitive to absorptions as small as 10^{-4} to 10^{-6} per pass, and one might expect similar sensitivity to gain. Our measurements have thus far been confined to the Ba + N_2O reaction and to wavelengths below 7400 Å. Thus, we have not yet checked the BaO[$A^1\Sigma, v'=1 \rightarrow X^1\Sigma, v''=7$] transition at 7900 Å, which has been predicted to have gain.[3]

Experimental Technique

The basic experimental layout is indicated in the following sketch.

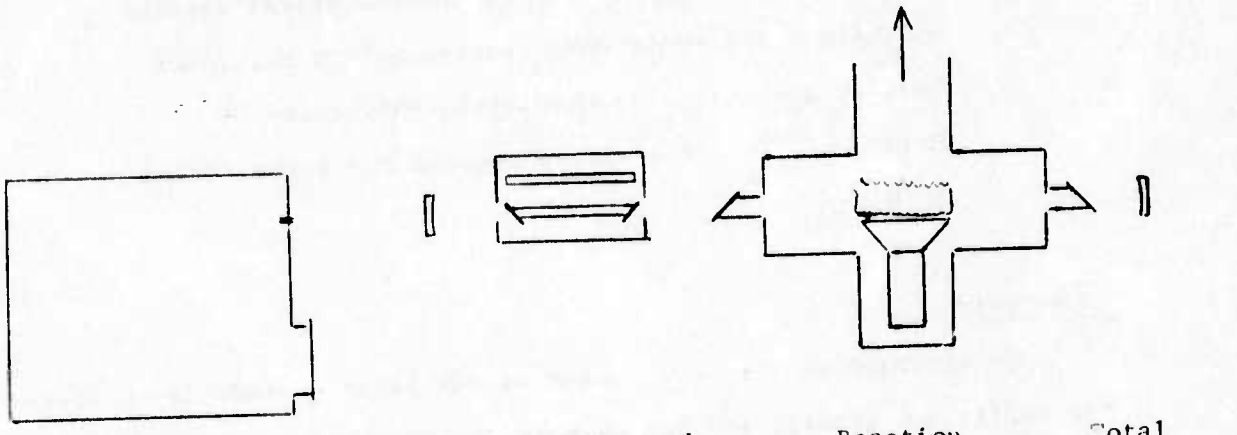

The dye laser was pumped by a linear flashlamp in an elliptical cavity, furnishing laser pulses of ~ 500 ns. The mirrors had 1-m concave radius of curvature, and were dielectric coated for total and for 95% reflection in the appropriate wavelength ranges. Wedged windows were used on both the dye cell and the reaction chamber to reduce etalon effects in the dye laser output. Spectra were recorded on a Jarrell-Ash, Model 78-460, 1-m spectrograph using Kodak high-speed infrared film. A 197-line/mm grating blazed for 3.7 μ was used in 7th to 9th order, giving dispersions of 3.2 to 4.5 Å/mm.

In the absence of intracavity absorption/gain effects, the dye laser output consists of a fairly smooth intensity distribution over approximately a 200 Å range. This broadband output was tuned by choice of dyes and by varying the dye concentration. Intracavity absorptions reduce the intensity at the absorbing wavelength, and intracavity gain enhances the intensity, each in proportion to the strength of the effect. Thus, effects due to the flame are detected by scrutiny of the dye laser spectrum. Since the laser has ample intensity to expose the film with

a single shot, a set of runs consists of a number of single laser shots, each taken at different flame conditions.

The burner was developed by C. R. Jones and H. P. Broida and loaned to us by Professor Broida. It consists of a 40 mm φ x 95 mm ceramic crucible containing Ba chips and heated by a cylindrical tube heater. Several layers of 60-mesh stainless steel screen were placed inside the crucible to provide a wick for increasing the evaporation surface area of the molten Ba. The crucible temperature, measured by an optical pyrometer, was typically 900° C. A transition section converts from cylindrical to a rectangular flame channel 0.8 cm x 10 cm. A tube extending into the crucible injects Ar carrier gas. The oxidizer is injected into the Ba + Ar flow from tubes attached to the 10-cm edges of the transition section. The flame is confined by side plates to a 1-cm-wide channel above the burner throat. The reaction chamber was connected to a 75 ℓ/sec Rootes pump system through a throttling valve. Test pressures, controlled through a combination of Ar bleed gas rate and throttle valve setting, ranged from 0.5 to 15 torr.

Results

Our initial experiments were aimed at detecting absorption from low vibrational levels of BaO($X^1\Sigma$) state. This was first accomplished on the $v'' = 0 \rightarrow v' = 4$ transition at 5350 Å. We next detected absorptions on the $v'' = 1 \rightarrow v' = 2$ and $v'' = 0 \rightarrow v' = 1$ transitions at 5864 and 5806 Å, respectively. These spectra, shown in Figure 1 (a)-(c) also show numerous absorptions on Ba transitions and, more surprisingly, an apparent enhancement on a Ba^+ transition, $Ba^+(6p\,^2P_{\frac{3}{2}} \rightarrow 5d\,^2D_{\frac{3}{2}})$. The lower level, $Ba^+(5d\,^2D_{\frac{3}{2}})$, is the lowest metastable level of the ion and thus seems a poor candidate for a transition with gain. Such a possibility cannot be discounted entirely, however, since pulsed discharges have produced such a laser.[4] When the run was repeated, the Ba^+ transition appeared in absorption and the $Ba(6p'\,^1P_1^o \rightarrow 5d\,^1D_2)$

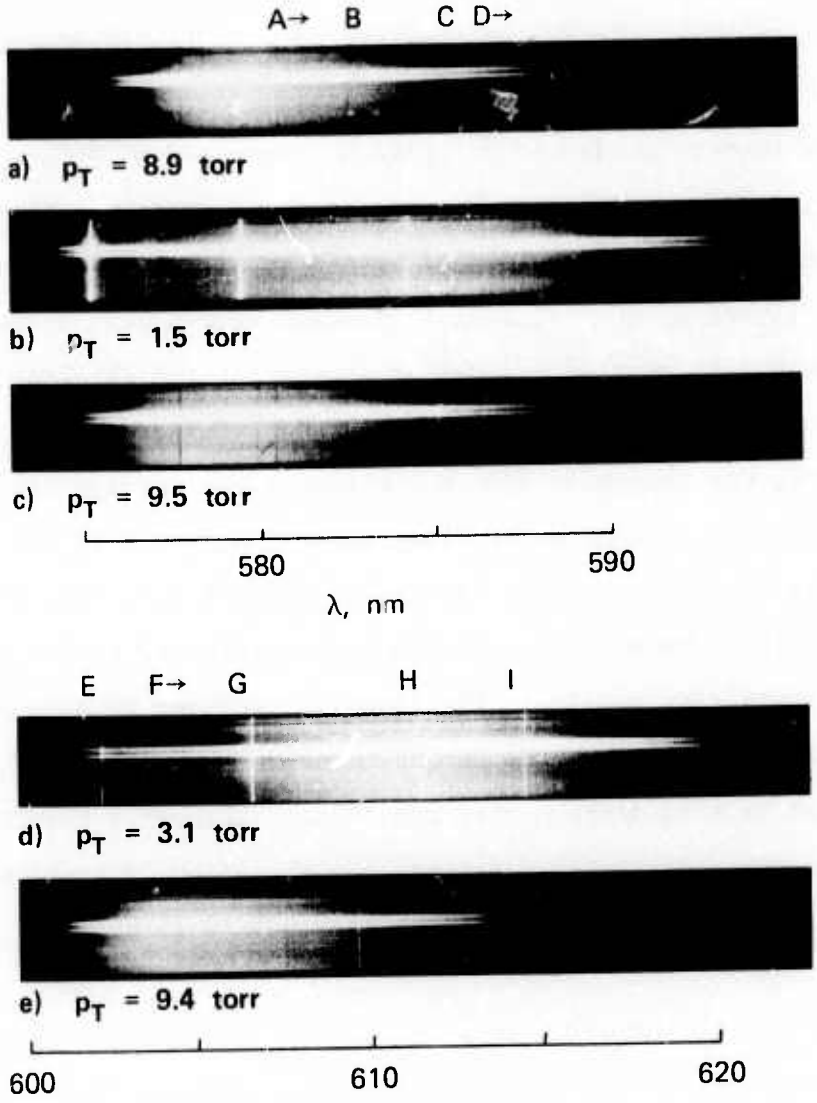

A: $BaO[A^1\Sigma,\ v' = 1 \leftarrow X^1\Sigma,\ v'' = 0]$

B: $Ba[6p'^1P_1^o \leftarrow 5d^1D_2]$

C: $Ba^+[6p^2P_{3/2}^o \leftarrow 5d^2D_{3/2}]$

D: $BaO[A^1\Sigma,\ v' = 2 \leftarrow X^1\Sigma,\ v'' = 1]$

E: $Ba[6p'^3P_0^o \leftarrow 5d^3D_1]$

F: $BaO[A^1\Sigma,\ v' = 1 \leftarrow X^1\Sigma,\ v'' = 1]$

G: $Ba[6p'^3P_1^o \leftarrow 5d^3D_2]$

H: $Ba[6p'^3P_1^o \leftarrow 5d^3D_3]$

I: $Ba^+[6p^2P_{3/2}^o \leftarrow 5d^2D_{5/2}]$

SA-3190-77

FIGURE 1 BROADBAND DYE LASER SPECTRA WITH INTRACAVITY Ba + N_2O FLAME

transition was enhanced. Again, the lower level is metastable. We do not believe these enhancements represent gain, and an alternative explanation is discussed below.

A laser probe covering 600 to 620 nm revealed enhancement on the second branch of the Ba^+ doublet, $Ba^+(6p^2P_{\frac{3}{2}} \leftarrow 5d^2D_{5/2})$, at 6142 Å, in addition to enhancements on numerous Ba transitions ending in the metastable $5d^3D$ levels and absorption on the $v''= 1 \rightarrow v'= 1$ band of BaO [Figure 1 (d), (e)]. Later probes revealed enhancement on the $Ba^+(6p^2P^o_{\frac{3}{2}} \leftarrow 6s^2S_{\frac{1}{2}})$ transition, where the lower level is the ground state of the ion, and very weak absorption on the BaO $v''= 5 \rightarrow v'= 1$ transition at 7175 Å, together with numerous atomic and ionic absorptions. The observed molecular absorptions, the enhancements, and atomic and ionic absorptions detected are summarized in Tables I through III, respectively. Surprisingly, we did not detect the BaO $v''= 4 \rightarrow v'= 0$ transition, although it falls in the same wavelength range as the $v''= 5 \rightarrow v'= 1$ transition and has a larger Franck-Condon factor. This suggests that the $BaO(X^1\Sigma)$ $v''= 5$ level may have a larger population than the $v''= 4$ level, in keeping with some of our earlier predictions.[5]

The intracavity absorption technique can be made quantitative by suitable calibration of intensity changes with known concentration of absorber, but our results are only qualitative, particularly in view of the nonreproducibility of experimental conditions from day to day and even from shot to shot. However, from past experience, Mr. Reilly estimates that the threshold for detection of absorption with his apparatus is about 5×10^{-4}/pass, and that the absorption in most of our cases is probably an order of magnitude stronger, or about 5×10^{-3}/pass. We have used the latter value, together with the appropriate transition probabilities for the absorptions observed, to calculate populations of the absorbing states. These calculations led to estimates of about 10^8 to $10^9/cm^3$ for the Ba and Ba^+ states and about $10^{12}/cm^3$ for the

Table I

Molecular Absorptions Detected
in Intracavity Dye Laser Experiments

Band Head λ_{Air} (Å)	$BaO(X\,^1\Sigma)$ v″	$BaO(A\,^1\Sigma)$ v′	Franck-Condon Factor
5349.7	0	4	0.16
5864.5	1	2	0.13
5805.2	0	1	0.043
6039.6	1	1	0.13
7175.2 (weak)	5	1	0.026

Table II

Atomic and Ionic States Giving Rise to Absorptions
in Intracavity Dye Laser Experiments*

Specie	Absorbing States
Ba	$5d\,^3D_{1,2,3}$
	$5d\,^1D_2$
	$6p\,^3P^o_{0,1,2}$
Ba^+	$5d\,^2D_{\frac{3}{2}}$
	$7p\,^2P^o_{\frac{1}{2}}$

*Enhancements listed in Table III are also attributed to absorbing states.

Table III

Enhancements Detected
in Intracavity Dye Laser Experiments

λ_{Air} (Å)	Specie	Lower State (E_ℓ, cm^{-1})	Upper State (E_u, cm^{-1})
4554.04	Ba II	$65\,^2S_{\frac{1}{2}}(0)$	$6p\,^2P^o_{\frac{3}{2}}(21952.42)$
5853.68	Ba II	$5d\,^2D_{\frac{3}{2}}(4873.85)$	$6p\,^2P^o_{\frac{3}{2}}(21952.42)$
6141.72	Ba II	$5d\,^2D_{5/2}(5674.82)$	$6p\,^2P^o_{\frac{3}{2}}(21952.42)$
6019.47	Ba I	$5d\,^3D_1(9033.99)$	$6p'\,^3P^o_0(25642.16)$
6063.12	Ba I	$5d\,^3D_2(9215.52)$	$6p'\,^3P^o_1(25704.14)$
6110.78	Ba I	$5d\,^3D_3(9596.55)$	$6p'\,^3P^o_2(25956.55)$
5826.28	Ba I	$5d\,^1D_2(11395.38)$	$6p'\,^1P^o_1(28554.26)$

BaO $v''= 0$ and $v''= 1$ states. The latter estimate assumes a rotational distribution such that 2% of the molecules in a given vibrational level absorb on the strongest transition. The atomic populations are about what we would expect for the metastable Ba levels based on our past results from emission measurements.[5] Likewise, the BaO $v''= 0$ and 1 concentrations are within reasonable expectations. To our knowledge, this is the first direct evidence of Ba^+ in these flames. The magnitude of the Ba^+ concentrations is surprisingly large.

The enhancements observed in our intracavity spectra must be interpreted with some care. While optimism would suggest that there was gain on these transitions, it is more likely that the enhancements result from anomalous dispersion effects in the flame. This refers to the fact that the index of refraction of an absorbing gas undergoes large excursions above and below the near unity value on the two wings of the transition. The strength of this index of refraction change increases with the strength of the absorption (or gain). If there is a gradient in the absorbing species, the resulting index gradients will create a lens that can alter the dye laser beam so that the laser intensity is increased at those wavelengths. This effect has been observed previously by Shank and Klein[6] and by Reilly,[7] and was explained by Shank and Klein. Under sufficiently high resolution, the transition should then appear as enhancements in the wings of the line and absorption on line center, as was the case in some of our spectra. Figure 1 (c) shows such a double enhancement; a microdensitometer trace of that feature is shown in Figure 2. Apparently the appearance of the feature depends on its strength and on the spectral resolution.

We conclude that the enhancements observed in our intracavity spectra are artifacts that reflect not gain but instead rather strong absorption on certain transitions. These absorptions are consistent with large populations of the metastable levels of Ba and Ba^+.

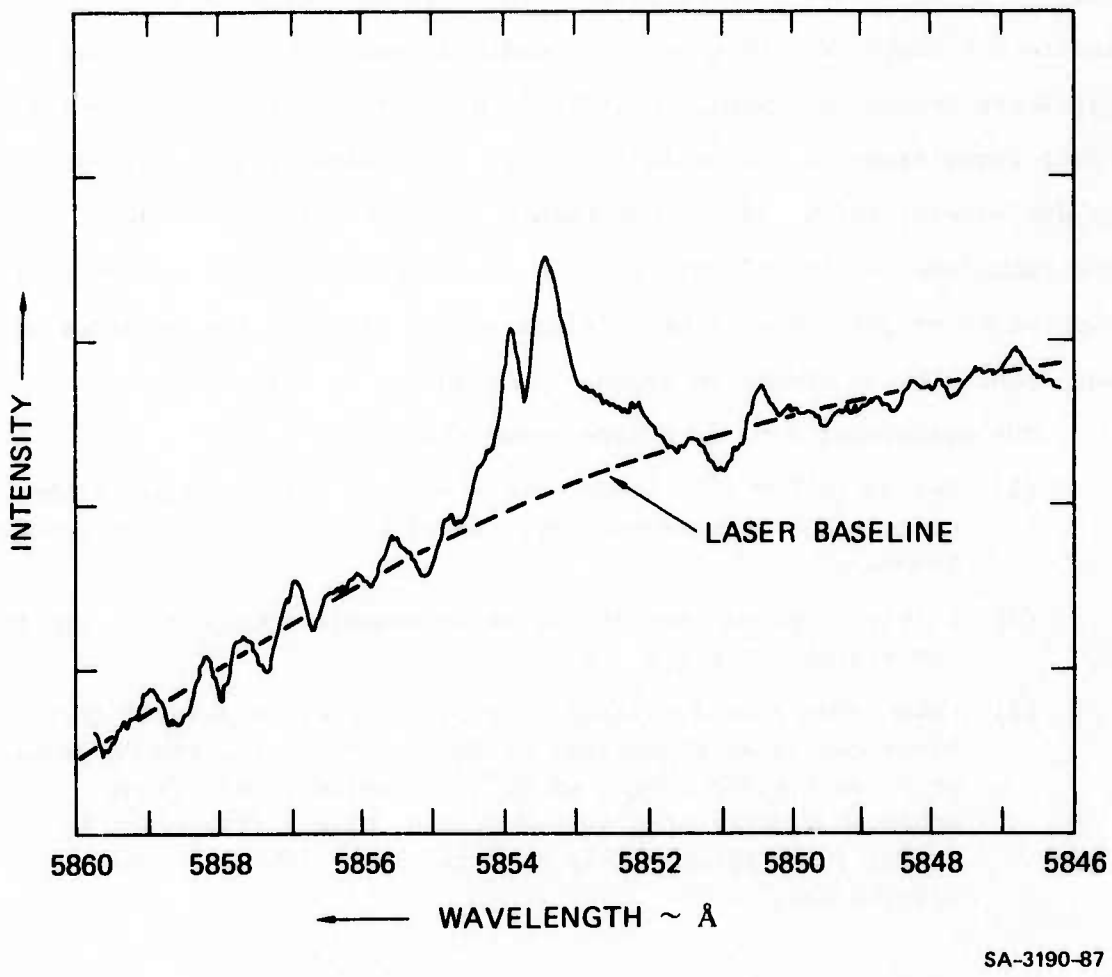

FIGURE 2 MICRODENSITOMETER TRACE OF ENHANCEMENT FEATURE ON 5853.7 Å Ba^+ LINE IN INTRACAVITY ABSORPTION SPECTRUM

Conclusions

Our intracavity dye laser absorption/gain measurements on the Ba + N_2O reaction, although limited so far, have been an informative supplement to emission spectroscopy studies. The technique should be developed further so that it can be a routine diagnostic tool for visible chemical laser development. The difficulties with its application are that: fairly long path length flames with high reaction rates are needed to generate detectable absorption/gain; many candidate laser transitions fall outside the wavelength range easily accessible by dye lasers; and not all enhancements indicate gain on a transition. The technique has the virtues of being able to specify the presence of absorption or gain on many transitions and to identify the presence of many nonradiating states in atoms, ions, and molecules.

Our measurements to date have shown that:

(1) The $BaO(A\,^1\Sigma \rightarrow X\,^1\Sigma)$ bands with $v' = 1$ and $v'' = 0 \rightarrow 5$ are either noninverted or have extremely small gain for our flame conditions.

(2) Fairly large concentrations of metastable levels of Ba and Ba^+ are present in the flame.

(3) Enhancements in dye laser intensity appear on several transitions ending on metastable Ba levels and on the ground level or on metastable levels of Ba^+. We believe that these enhancements are artifacts due to anomalous dispersion by fairly large concentrations of the lower levels of those transitions.

Background

Because several of our earlier studies indicated that BaO^* emission is strongly quenched by Ba atoms, we performed a series of measurements in a heat-pipe-oven reactor (HPOR) in an attempt to quantify this effect. The measurement technique and many experimental results were described in our last semiannual report.[5] Those results included photon yields for both atomic (Ba^*) and molecular (BaO^*) emission as a function of metal density and total pressure. They also included extensive analysis of the population distributions and photon yield distributions for the atomic Ba^* emission. During this period, we repeated the experiments over an extended temperature range. New results for BaO^* emission as a function of metal and total pressures are reported here.

Experimental Technique

Briefly, the HPOR provides a large region of uniform and essentially static Ba density. The total pressure in the HPOR is set by adjusting the buffer gas (Ar) pressure outside the oven; in the oven, this pressure is the sum of Ba and Ar partial pressure. In the pure heat-pipe mode, only Ba is present in the oven; in the mixed gas mode, both species are present. In the latter case, which was always the experimental situation, the Ba pressure was set by the externally imposed oven temperature, with Ar constituting the difference. We thus presume to know the Ba concentration based on the vapor pressure curve for Ba and the oven temperature. In fact, both the vapor pressure dependence and the oven temperature are somewhat uncertain. In particular, we have reevaluated the oven temperature measurements and have reassigned Ba densities for the data reported previously. The original and revised Ba concentrations are as follows:

N(Ba) ~ cm^{-3} (reported previously)	N(Ba) ~ cm^{-3} (revised)
2.4×10^{13}	2×10^{14}
6.0×10^{13}	6×10^{14}
1.9×10^{14}	1×10^{15}
4.7×10^{14}	1.5×10^{15}

The revised values are used here in reporting molecular photon yields. A factor of two uncertainty still exists in the values of metal density.

The oxidizer (N_2O) was introduced into the Ba zone through a quartz capillary, resulting in a spherical diffusion flame with Ba in excess. By independent adjustment of oven temperature and Ar pressure, photon yield measurements were obtained as functions of [Ba] concentration and p_{total}.

Results

Figure 3 shows the earlier molecular photon yields[5] together with the recent results. The "flowing system results" are a composite of our own work and work from the laboratories of H. P. Broida (UCSB) and H. B. Palmer (Penn State) in which flowing jets of Ba and N_2O interact. The marked reduction in molecular photon yield with [Ba] was already noted in the earlier data. The surprising fact of the new results is that photon yields exceed those of the "flowing systems" at low pressures, by as much as a factor of two in some cases. This emphasizes a problem inherent in making photon yield measurements at low pressure, namely, that all the minor species in the reaction may not be consumed within the field of view. The larger region of uniform metal density in the present experiments should eliminate that problem, and probably accounts for the higher yields compared with flowing system results.

These new results imply that, at best, the kinetic models that we and others have devised to fit the Ba + N_2O results (based entirely on the flowing system curve) have produced the wrong values of pertinent parameters and, at worst, that the kinetic models are totally wrong. The latter

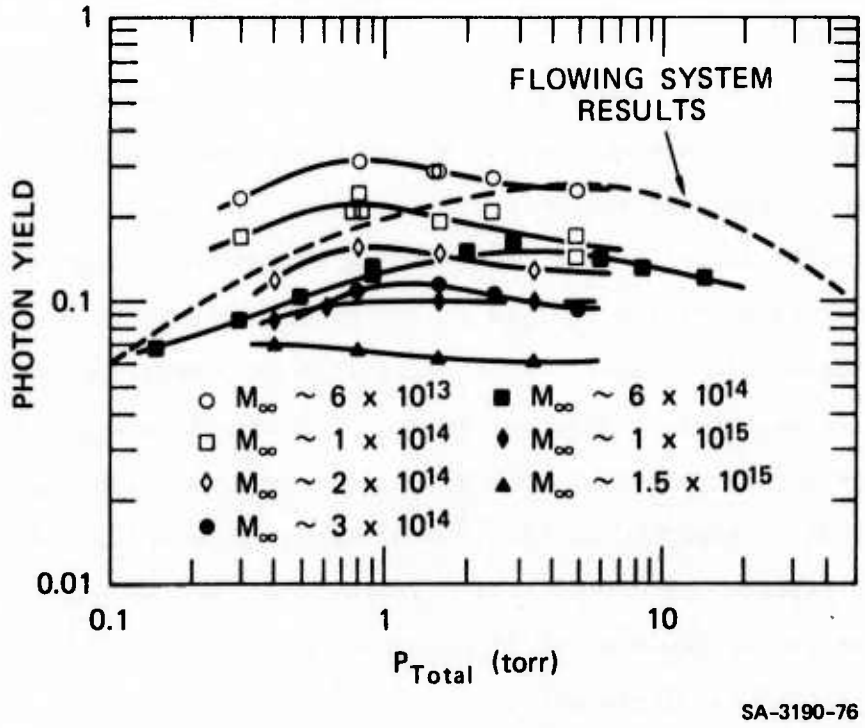

FIGURE 3 EFFECTS OF METAL ATOM CONCENTRATION ON Ba + N_2O PHOTON YIELD

prospect seems more likely when we observe that metal density appears in Figure 3 to be a more important parameter than total pressure. To elucidate this point, Figure 4 plots the photon yields as a function of Ba concentration at four values of p_T. There is considerable scatter in both Figures 3 and 4, but the data are nearly collapsed into a straight line in the second plot. The slope of the line corresponds to a $[Ba]^{-\frac{1}{2}}$ dependence, and variations about the line are less than approximately 60%.

Conclusions

The results of Figure 4 substantiate the importance of metal atom concentration in determining the photon yield and suggest that it may, in fact, be the dominant variable for Ba + N_2O. One could then explain some of the variations with p_T in the flowing system results by suggesting that the metal concentration is tied to the total pressure in a unique way (e.g., through diffusion). This suggestion is consistent with the observation by Felder et al.[8] that the photon yield for Ba + N_2O did not vary for argon pressures from 5 to 120 torr in their flow tube experiments. We are left to explain the $[Ba]^{-\frac{1}{2}}$ dependence (pure metal atom quenching would be expected to give a $[Ba]^{-1}$ dependence), and we note finally that extrapolation of the results of Figure 4 to $[Ba] < 6 \times 10^{13}$ could give photon yields well above 30%.

We are still working toward a new kinetic model that explains these HPOR results. Until that is achieved, we can only express considerable uncertainty about the mechanisms of chemiluminescence in this and other reactions.

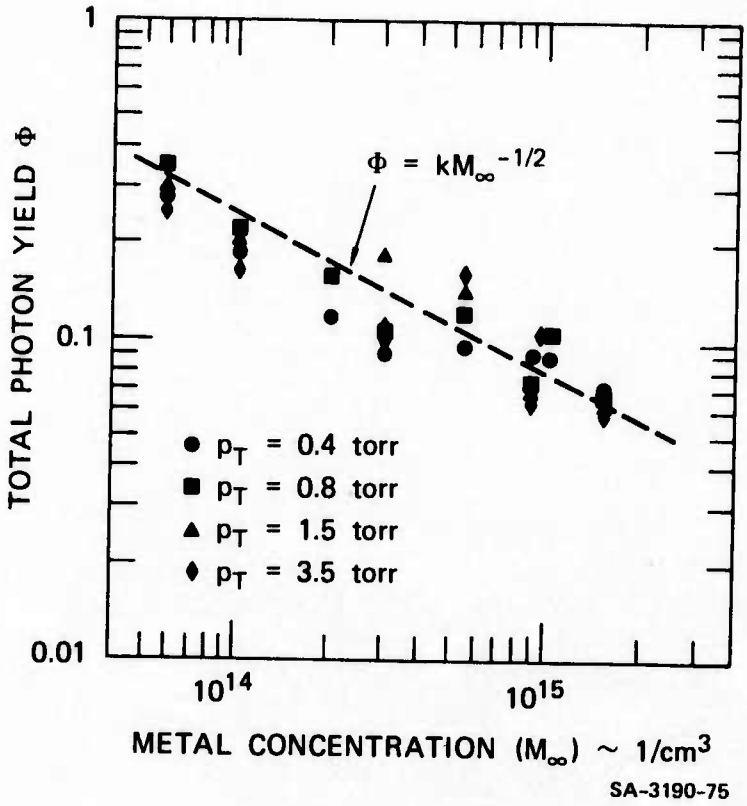

FIGURE 4 PHOTON YIELDS FOR THE Ba + N_2O REACTION AS A FUNCTION OF Ba CONCENTRATION

EFFECTS OF ELECTRIC FIELDS ON Ba + N_2O FLAMES

Background

We have postulated that chemiluminescence from metal atom plus oxidizer reactions is a two-step process consisting of production of high vibrational levels, $MX^{\ddagger\ddagger}$, of the newly formed molecule, followed by intersystem transfer leading to radiating states, $MX^{\ddagger\ddagger} + N \rightleftarrows MX^{*} + N$, in collisions with the background gas. Collisions will also lead to vibrational relaxation, $MX^{\ddagger\ddagger} + N \rightarrow MX^{\ddagger} + N$, which reduces the photon yield and could fill the lower vibrational levels so that any population inversion would be destroyed. If this premise is correct, one might expect that imposition of an electric field could enhance the photon yield, since heated electrons could cause efficient intersystem crossing without attendant vibrational relaxation (in fact, vibrational excitation might be more likely). A second reason to hope for enhanced photon yields in flames with discharges is that the discharges will produce Ba metastable atoms (^1D and ^3D states), and reactions of Ba^M might lead to direct production of BaO^* with a higher efficiency than the reaction of ground state atoms. Finally, we have observed very bright emissions from flames during transient "accidental" low-voltage discharges in our previous photon yield studies.

To investigate these possible effects, we studied the emission from a Ba + N_2O + Ar flame with applied microwave fields [industrial band (2.45 GHz) and X-band (9 GHz)], dc fields ("predischarge"), and dc glow discharges.

Experimental Technique

The experimental apparatus and techniques for carrying out the measurements are the same as those described for our previous photon yield measurements.[1] Briefly, the barium is vaporized in a high temperature oven and carried into the reaction region by argon. Ba is the excess specie, with the N_2O introduced into the center of the metal jet through a capillary tube. The oxidizer is completely consumed in an approximately spherical diffusion flame centered on the capillary tip. The light output is measured from 2000 Å to the edge of the photomultiplier response at about 8600 Å.

Microwave Results

The flame region was bathed in 2.45-GHz (industrial band) microwaves by mounting a microwave horn inside the vacuum system so that it faced the flame region from the side. The power is estimated to be 10 W, spread out over a 4-inch circular region in the flame plane. The microwave field causes the BaO bands to decrease in intensity, especially at longer wavelength. Figure 5 shows this decrease at a pressure of 1.3 torr. The structured $A^1\Sigma$ emission and the $A'^1\Pi$ pseudo-continuum show the same amount of decrease in the various wavelength regions. This decrease ranges from 15% at 4500 Å to 70% at 8000 Å. This decrease was unexpected, since the microwave field should increase interstate mixing without affecting the competing vibrational relaxation. The shift toward shorter wavelengths indicates that lower vibrational levels of $BaO(A^1\Sigma)$ are removed to a greater extent than the higher levels.

These microwaves also produced nitrogen second positive emission ($C^3\Pi \rightarrow B^3\Pi$). When no metal or N_2O was present, we saw these same N_2 bands, along with OH bands; these both occur readily as impurities.[9] In addition, many argon lines appeared in the regions 3950 to 4500 Å and 7380 to 8700 Å.

Experiments with 2.45-GHz microwaves were terminated because several microwave cables melted in the vacuum, even with water cooling. Microwaves

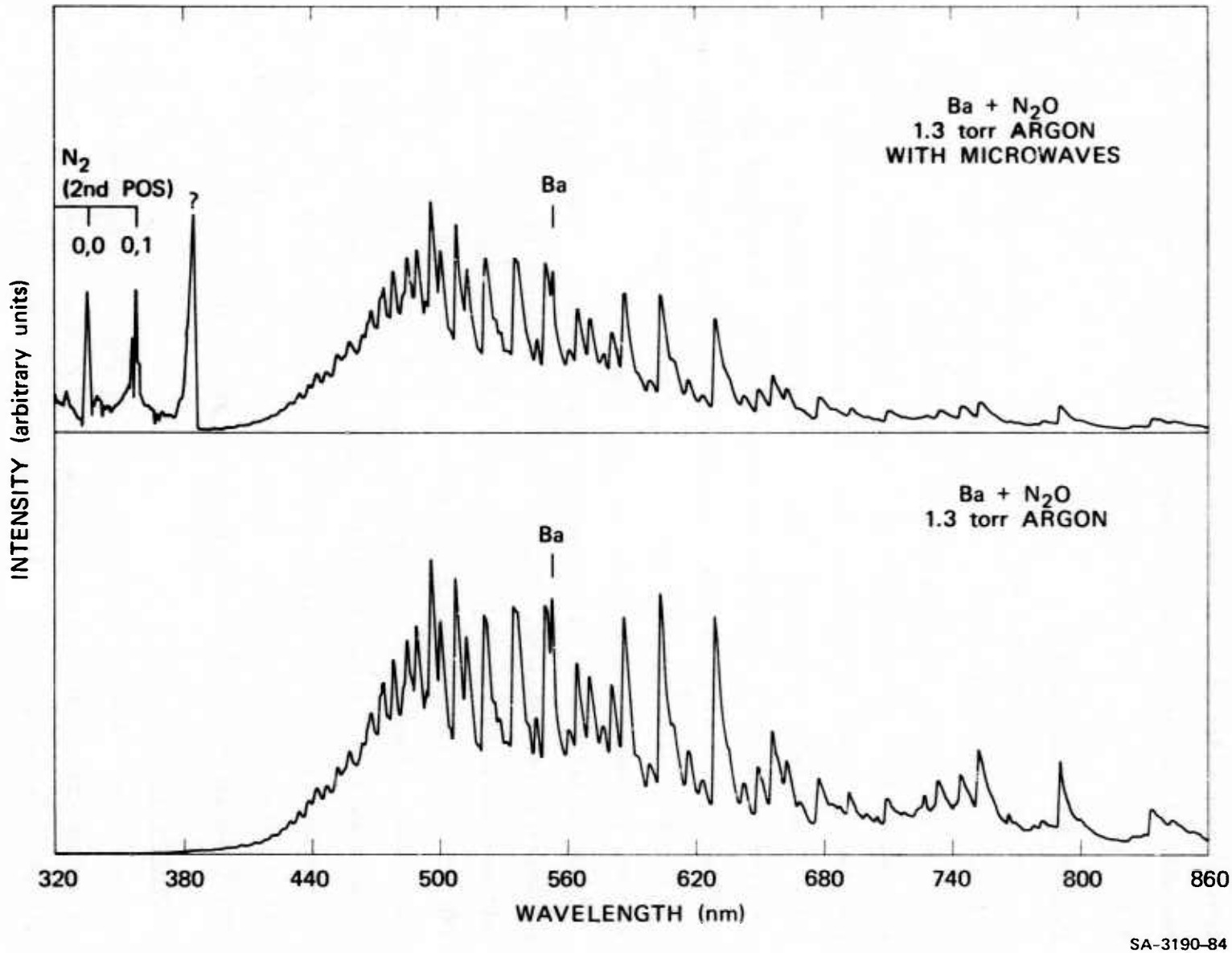

FIGURE 5 CHEMILUMINESCENCE SPECTRA OF THE Ba + N_2O REACTION WITH AND WITHOUT 2.45 GHz MICROWAVES

at approximately 9 GHz (X-band) were then beamed into the flame region from an open-ended piece of ½ in. by 1 in. waveguide ending ½ in. from the side of the flame. These showed no effect on the flame, even with 6 W of power.

DC Glow Discharge Results

An electric discharge was maintained in the flame region, using the oven for one electrode and a brass rod inserted axially (opposite the oven) to the end of the flame zone as the other electrode. Discharges were run at approximately 350 V and 15 mA. Typical results for the oven positive are shown in Figure 6. Note that the runs shown are with and without oxidizer. Runs without the discharge were similar to the bottom spectrum in Figure 5. With the discharge present, no BaO emission was observed regardless of oxidizer concentration. Rather, the emission consisted mostly of Ba^* and Ar^* lines. Again, both OH and N_2 bands were present, including some N_2 bands not seen before.

Both polarities of discharge were tried. With the oven negative, Ba^* emission was enhanced. The Ba^* populations tended to follow a Boltzmann distribution with an electronic temperature of approximately $3000^{\circ}K$. A few states lie off this curve, but have large variation from run to run. There was no significant difference in either the barium or argon lines when oxidizer was added. With the oven positive, only a few barium lines were present. In this case, the addition of N_2O caused both the barium and argon lines to enhance in the regions from 3850 to 4500 Å and above 6650 Å, and to quench in the middle wavelengths.

DC Predischarge Results

When the voltage was decreased to about 200 V, the current dropped several orders of magnitude and became very voltage sensitive. The runs with and without this electric field showed only minor changes, as indicated in Figure 7 for a 200 V, 90 μA case. There was no change in

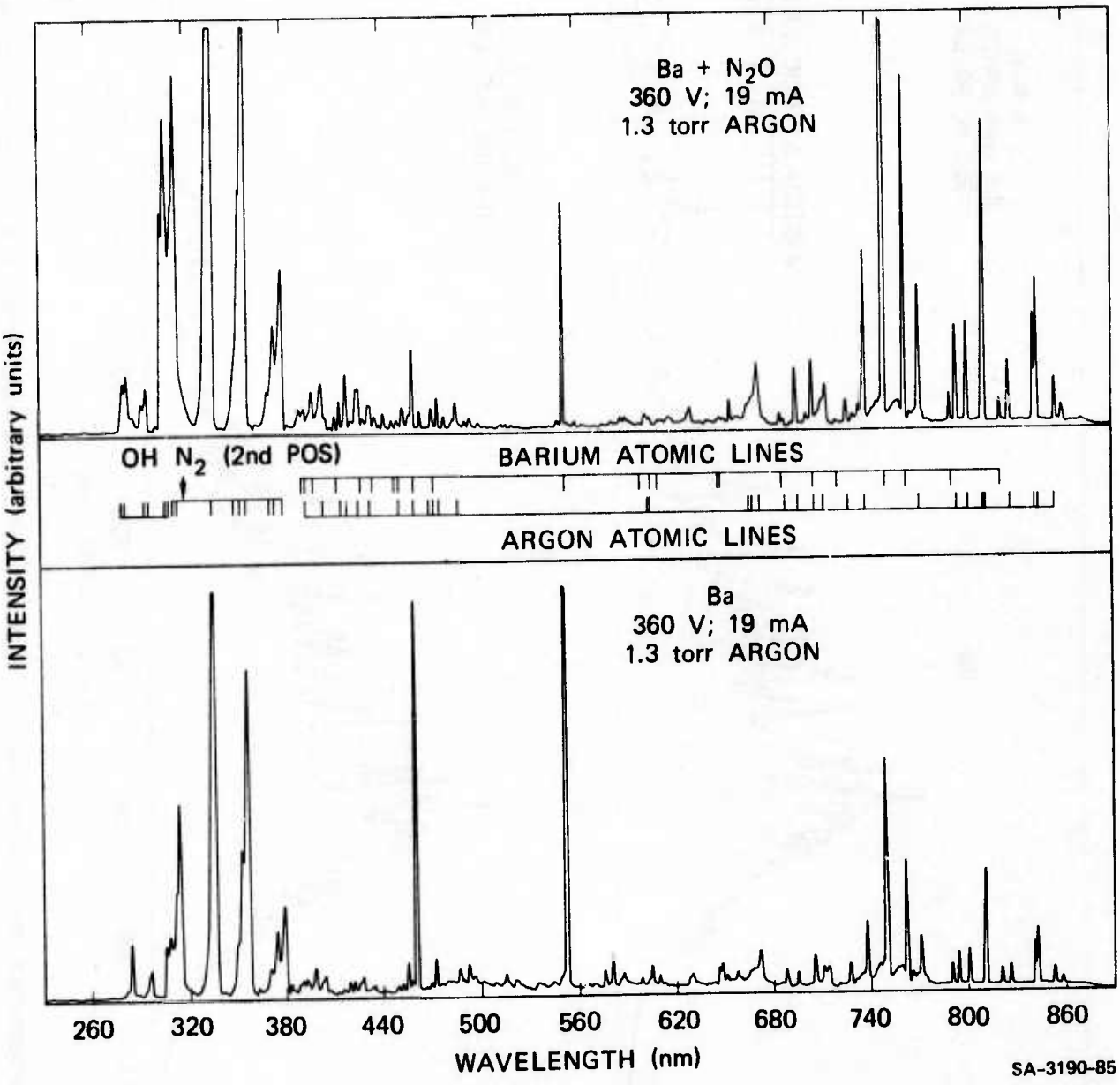

FIGURE 6 CHEMILUMINESCENCE SPECTRA OF Ba + N_2O AND Ba IN THE PRESENCE OF AN ELECTRIC DISCHARGE

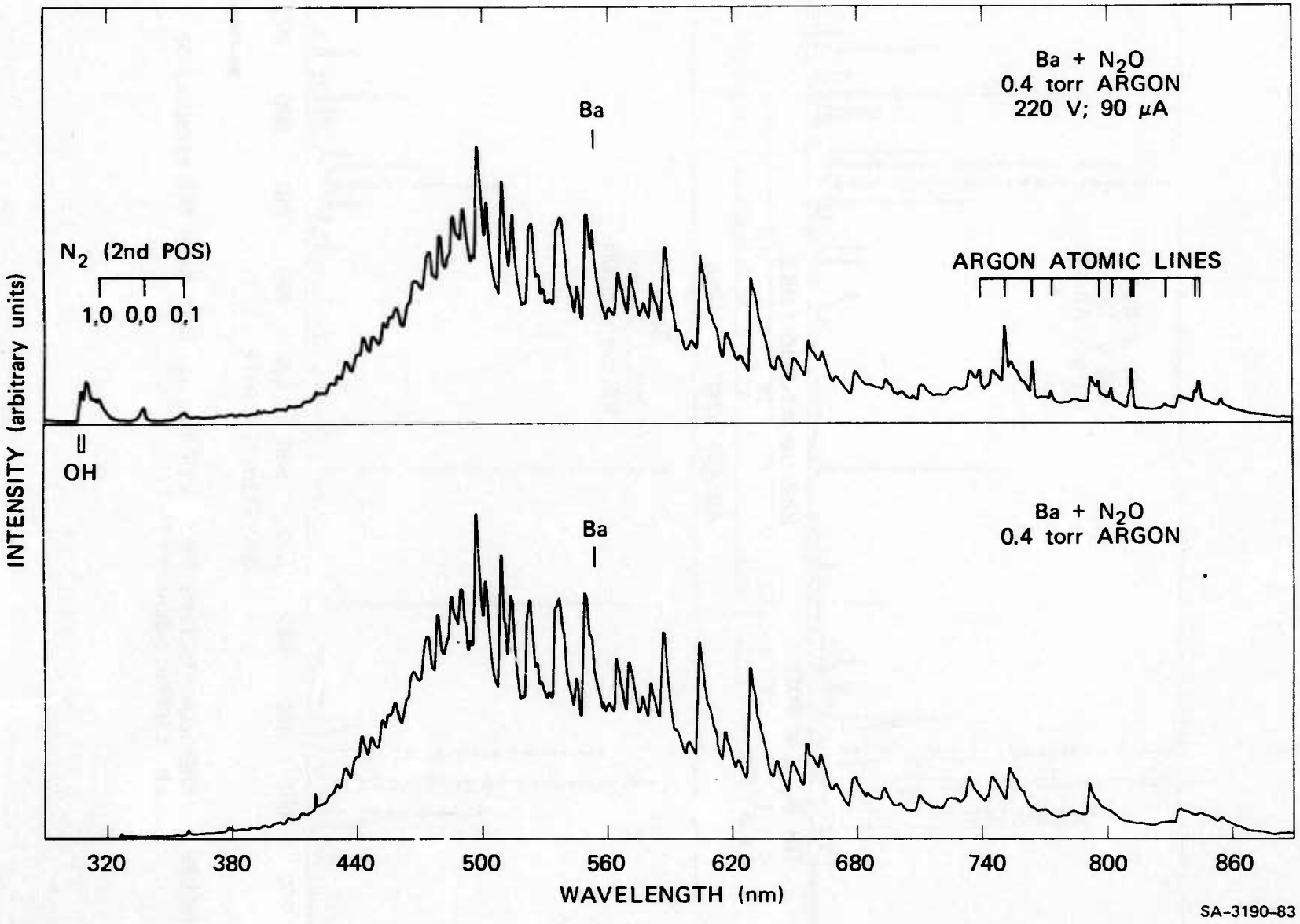

FIGURE 7 CHEMILUMINESCENCE SPECTRA OF THE Ba + N_2O REACTION WITH AND WITHOUT A PREDISCHARGE POTENTIAL

the BaO bands and only minor enhancement of the barium 5535 Å line and of several of the argon lines between 7100 and 8600 Å. The N_2 and OH impurity bands were again present when the voltage was on.

Conclusions

Since the results of these experiments were quite different from those we expected, we did not carry out extensive variations of the experimental parameters or make new diagnostic measurements. The departure from normal emission correlates at least roughly with field strength, with weak fields enhancing a few atomic lines, medium fields reducing BaO^* emission and exciting more atomic lines, and the strongest fields eliminating BaO^* altogether. There are three possible causes for these effects:

(1) Removal of N_2O as a reactant

(2) Removal of Ba as a reactant

(3) Quenching of $BaO^{\ddagger\ddagger}$ and BaO^* to prevent emission.

Of these, removal of Ba by ionization seems most likely. However, the presence of Ba^* emission indicates that some atomic Ba is present to react. Thus, this effect might be coupled with quenching of BaO^*. In spite of our preconceived ideas, the fact that different vibrational levels of BaO^* disappear at different rates seems to indicate that the emission process of BaO^* is being interrupted after the reaction of Ba and N_2O. Alternatively, reaction of Ba^M metastables could produce more energetic BaO^* than reaction of Ba ground state (which would shift the emission to the blue as we observed), but the total reaction rate could be reduced by Ba ionization. In any case, these results do not encourage the prospects for a hybrid chemical-discharge BaO laser.

SHOCK TUBE STUDIES

Background

Studies of reactions of metal atoms with oxidizers have always been troubled with two basic experimental problems. The first is the difficulty of evaporating sufficient quantities of many metals of interest, and the second is mixing metal atoms and oxidizers rapidly enough to reach the reaction rates characteristic of laser threshold. During our flame experiments, quenching of molecular emission by the reactants also appeared as a serious problem. A fourth problem is that vibrational relaxation in the molecular ground-state manifold can fill the lower vibrational levels and destroy potential population inversions.

The first problem might be alleviated by using volatile encapsulated metal compounds (carbonyls or alkyls) of low-volatility metals (an approach we tried unsuccessfully earlier in flame studies,[10] where it appeared that gradual decomposition of the metal compound and partial oxidation of the fragments precluded achievement of free metal atoms). The problem of mixing can be avoided by premixing the reactants. The problems of reactant quenching and vibrational relaxation might be alleviated by using rapid pulsed reactions, since the reactants will disappear as product molecules appear and since the reaction might be rapid on the time scale of vibrational relaxation. These experimental objectives may be achieved through the study of premixed, pulsed reactions of volatile metal compound plus oxidizer in a shock tube. The reaction is initiated in this case by the rapid heating produced by the incident shock wave.

This approach is somewhat different from other shock tube chemical laser studies. Johnson and coworkers[11] at Xonics are using the shock tube to vaporize metal particulates; the metal atoms are then mixed with

oxidizer downstream of a supersonic expansion nozzle. Cool and coworkers at Cornell University use shock tube heating to vaporize and pressurize metal compounds; again the metal compounds are mixed with oxidizer downstream of a supersonic expansion nozzle, and the reaction is then triggered with an e-beam discharge [T. Cool, private communication]. Problems with our present approach include stability and compatibility of reactants, kinetic interference from the fragments of the encapsulating metal compound, and the speed of the reaction relative to observation time and/or vibrational relaxation time.

Experimental Technique

Experiments are being carried out in a 5-cm I.D. stainless steel shock tube with a 4-m driven section and a 1-m driver. Shock waves are initiated by spontaneous rupture of pre-scribed diaphragms by cold He or N_2 driver gas. The test gases consist typically of 5% encapsulated metal in Ar and 5% oxidizer in Ar admitted to the shock tube simultaneously through a single orifice after passage through parallel flow meters and valves. The initial test gas pressure is typically 5 to 8 torr; the shock tube is pumped to $\sim 10^{-5}$ torr before filling. Because of the toxicity of the carbonyls, the test section and gas handling system are in a separate, vented room, and filling is carried out remotely. Shock speeds are measured by thin-film platinum heat gauges. Frozen gas conditions behind the incident shock range from $\sim$ 1000 to 3000^{o}K and $\sim$ 0.1 to 0.5 atmospheres; reflected shock temperatures range as high as 7000^{o}K.

The emission from each shock wave was monitored by a Princeton Applied Research optical multichannel analyzer (OMA) coupled to a Jarrell-Ash, Model 82-410, ¼-m spectrograph and by a Heath, Model EU-700, 0.35-m monochromator with an RCA 31034 phototube. By gating of the OMA, broadband spectra at discrete time intervals were obtained; the monochromator gave time histories of emission at discrete wavelengths. By varying the grating in the J/A spectrograph, we could obtain spectral coverage of 175, 350, or

4000 Å in a single shot. The detector is sensitive rom 3000 to 6500 Å. Gating of the OMA detector and storage of data in the OMA memory were triggered by the incident shock wave; exposures ranged from 10 to 100 μsec.

Results

The first system examined was $Ni(CO)_4 + N_2O + Ar$. Our first consideration was the decomposition rate of the carbonyl. We had previously estimated that the splitting off of the carbonyls would be sequential and that the last step would be rate limiting, with an estimated rate of $10^{-(9+6100/T)}$ cm^3/sec [Dr. S. W. Benson]. For our conditions, this corresponds to a decomposition time of a few microseconds or less. We attempted to measure this rate by observing density gradients behind the incident shock wave using the laser schlieren technique, but we could find no difference in the schlieren signal with and without $Ni(CO)_4$ added to the Ar bath. We concluded that the decomposition was complete less than 1 to 2 μsec behind the shock front.

Emission behind the incident shock wave was dominated by atomic Ni lines at higher temperatures and by an unresolved continuum in the red and near IR that could be blackbody emission. No clear evidence for molecular emission was obtained. Very strong Ni line emission was observed behind the reflected shock. This Ni radiation is probably thermally excited in all cases. The NiO(A-X) bands are in the near IR, outside the sensitive range of the OMA, so it was difficult to determine the presence of this emission. The monochromator detected emission throughout the appropriate spectral range, but there was no correlation of intensity with band head locations. The NiO(B-X) system in the visible did not appear; the $Ni + N_2O$ reaction is exothermic enough to populate the NiO(A) state, but not the (B) state.

We next studied briefly the $Ni(CO)_4 + NF_3 + Ar$ system. In this case, the NiF(A-X) emission is in the visible, but the $Ni + NF_3$ reaction is not exothermic enough to populate the NiF(A) state directly. We did observe NiF(A-X) emission of moderate intensity on the OMA. Calculations indicate that the emission is probably due to thermal excitation of NiF to the (A) state.

The third system studied was $Sn(CH_3)_4 + N_2O + Ar$. The $Sn + N_2O$ reaction is exothermic enough to populate several SnO^* excited states, each of which radiates in the visible. Furthermore, $Sn + N_2O$ has been found to have high photon yields and low quenching rates in flame studies [A. Fontijn, private communication]. Our emission measurements were confined to the incident shock region and covered the 1000 to 3000°K temperature range. We do not see the SnO(a→X,A→X) bands that we anticipated, but only moderately weak SnO(D→X) emission (notation of Rosen or Suchard), and perhaps some SnO(C-X) bands, although these cannot be clearly separated from the (D→X) system. The (D-X) emission increases with temperature approximately as $e^{-5,000\ cm^{-1}/kT}$, as though the reaction producing the emission had a 5000 cm^{-1} activation energy or as though the (D) state were being populated thermally from a reservoir 5000 cm^{-1} below the (D) state energy. In fact, the SnO (B and C) states are ~ 5000 cm^{-1} below the D state, but we do not see radiation from those states. Fontijn (private communication) reports that the SnO(a) emission disappears and SnO (C and D) emission appears in flames at temperatures above 1000°K, and attributes the change to thermal decomposition of N_2O and subsequent three-body recombination $Sn + O + M \rightarrow SnO$ (C and D) + M. This seems less likely in our case since N_2O decomposition times are long compared with observation times. That rate (for N_2O in Ar) is:[12]

$$k = 8.3 \times 10^{-10} \exp(-58,000/RT)\ cm^3/sec \quad ,$$

which gives decomposition times from 20 μsec to ~ 1 sec for the conditions of these experiments.

In an attempt to explain the paucity of radiation from the $Sn(CH_3)_4 + N_2O$ system, we have plotted in Figure 8 several characteristic times for decomposition, reaction, radiation, and vibrational relaxation as a function of temperature behind the incident shock wave. The N_2O decomposition rate was listed above. The $Sn + N_2O$ reaction rate has been measured by Felder and Fontijn.[13] The radiation rate is an estimate for $SnO(a^3\Pi)$ based on measurements in matrices.[14] The decomposition rate for $Sn(CH_3)_4$ is an estimate based on unimolecular decomposition theory and assuming a 70 kcal/mole bond strength for splitting off the first methyl radical [calculation by Dr. D. M. Golden, SRI]. The vibrational relaxation rate for SnO ($v'' = 1 \rightarrow v'' = 0$) is based on the correlation of Millikan and White,[15] and the value for high vibrational levels is arbitrarily chosen as a factor of 10 faster (harmonic oscillator theory predicts that the rate is proportional to v, but anharmonicity reduces the dependence somewhat).

In contrast to the case for carbonyls, we now find that decomposition of the alkyl is probably quite slow and, in fact, may limit the availability of Sn atoms for reaction below about 1500°C. However, the temperature range may be limited to less than ~ 2000°K by the fact that the equilibrium for $SnO(a^3\Pi) \rightleftarrows Sn + O$ is shifted almost totally toward atoms at 2000°K and above. Thus, one might expect maximum SnO(a) emission at temperatures between 1500 and 2000°K, in contrast to our experimental observations.

Conclusions

The results obtained to date in premixed, pulsed shock tube chemiluminescence studies must be regarded as disappointing, with much less molecular emission observed than we had hoped for. However, we will continue to study the $Sn(CH_3)_4 + N_2O$ system in an attempt to understand the processes taking place so that we might achieve operating conditions that will yield more promising results.

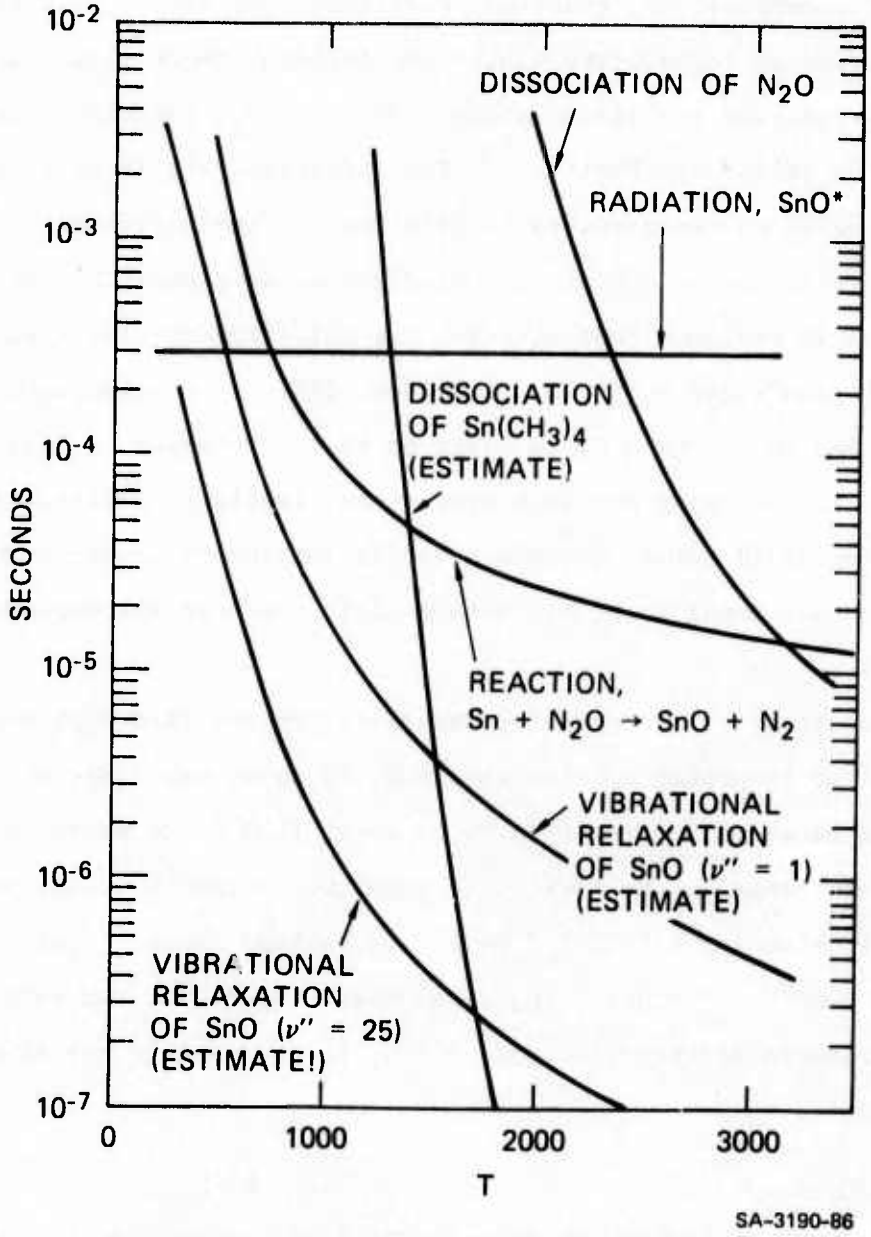

FIGURE 8 CHARACTERISTIC TIME CONSTANTS FOR SHOCK-HEATED $Sn(CH_3)_4 + N_2O$

$[N_2O] = 5 \times 10^{16}$

$[Ar] = 10^{18}/cm^3$

PROSPECTS FOR CHEMICALLY PUMPED ATOM ASSOCIATION LASERS

Background

The possibility of a molecular laser produced by the association of radicals:

$$A + B + M \rightleftarrows AB^* + M$$

$$AB^* \rightarrow AB + h\nu$$

(where M is a third body) was first suggested by R. A. Young[16] in 1964, based on his extensive experience with flowing afterglow photochemistry. Young estimated that atom concentrations of $\geq 10^{16}/cm^3$ could lead to population inversions sufficient for lasing. This approach was considered again in 1965 by Shuler, Carrington, and Light,[17] but from then until recently it received little attention, probably because of the difficulty of achieving the required atom concentrations in electrical discharge devices. For about the last two years, atom association reactions have received renewed interest from people who were aware that a shock tube can produce atom concentrations of $10^{19}/cm^3$ or more in the reflected shock region. Rapid expansion of this hot, high pressure, highly dissociated gas to lower densities and temperatures (say, $T = 2000^oK$, $p \sim 1$ atm, $N_{atoms} \sim 10^{18}/cm^3$) shifts the equilibrium back toward recombination and might lead to realization of a chemically pumped atom association laser. This shock-tunnel approach is currently under investigation in France[18] and the USSR,[19] and it is worth reevaluating the prospects for development of such a laser. It should be noted that many of the e-beam lasers currently under development involve association of atoms [e.g., $Xe + O(^1S) + M \rightarrow XeO^* + M$],[20] and so in some sense fall in this class. However, the pumping step in those systems critically involves electrons, and we exclude them from this discussion.

The critical factor to add to the evaluations of 11 and 12 years ago is the high rate of quenching of excited molecules by the atoms involved

in their formation [e.g., $O_2(A^3\Sigma_u^+) + O \rightarrow O_2(X^3\Sigma_g^-) + O$],[21] which frequently is near gas kinetic. These rates were not known at the time of the earlier studies. Second, in the shock tunnel environment, the recombination rate is reduced by the high temperatures, and the branching rates for formation of excited states may be different from those at room temperature and relatively low pressure. We will consider the following homonuclear diatomic cases that have been suggested as candidate reactions:

$$Br + Br + M \rightarrow Br_2(A^3\Pi_{1u}) + M$$

$$Cl + Cl + M \rightarrow Cl_2(A^3\Pi_{0_u^+}) + M$$

$$O + O + M \rightarrow O_2(A^3\Sigma_u^+) + M \quad .$$

Analysis

The full computation of the combined fluid dynamic and chemical kinetic properties of the shock-heated gases as they undergo rapid expansion is a lengthy and time-consuming process. However, we can use simplified procedures to estimate upper limits to the excited molecular populations that might be achieved. First, we assume $T \sim 4000^oK$, $p \sim 20$ atm, and 50% dissociation as reasonable reflected shock conditions [$N_A \sim 1.5 \times 10^{19}/cm^3$, $M \sim 3 \times 10^{19}/cm^3$]. Next we assume expansion to Mach number ~ 2.5 with frozen chemistry, so that $T \sim 2000^oK$, $p \sim 1$ atm, $M \sim 3 \times 10^{18}$, and $N_{A_o} \sim 1.5 \times 10^{18}/cm^3$]. This will surely give an upper limit for the number of atoms available for three-body recombination (this estimate exceeds the critical atom density deduced by Young by two orders of magnitude). We now consider the recombination process without further gas dynamic effects.

The rate of formation of excited molecules (neglecting collisional re-dissociation of the newly formed molecules) is

$$\frac{d(N_M^*)}{dt} = k_R^*(N_A)^2(M) - N_M^*[A + k_Q(N_A)] \quad , \qquad (1)$$

and the rate of disappearance of atoms is

$$\frac{d(N_A)}{dt} = -2k_{R_T}(N_A)^2(M) \quad , \tag{2}$$

where (N_A), (N_M^*), and (M) are the concentrations of atoms, excited molecules, and third bodies, respectively; k_R^* and k_{R_T} are the three-body recombination rates for excited molecules and all molecules, respectively; A is the radiative rate of excited molecules; and k_Q is the rate of quenching of excited molecules by atoms. Equation (2) can be solved explicitly for the time history of atoms, and this function can then be inserted in equation (1). A simpler approach is to divide (1) by (2). If we define the parameters

$$y = N_M^*/N_{A_o} \quad , \qquad x = 1 - N_A/N_{A_o}$$

$$B = k_R^*/2k_{R_T} \quad , \qquad C = k_Q/2k_{R_T}(M) \quad , \qquad D = A/2k_{R_T}(M)(N_{A_o})$$

where N_{A_o} is the initial concentration of atoms, we obtain

$$\frac{dy}{dx} = B - \left[\frac{C}{1-x} + \frac{D}{(1-x)^2}\right]y \quad . \tag{3}$$

Unfortunately, this still does not admit a simple closed form solution. However, two approximate solutions can be obtained. The first follows from graphical considerations of equation (3) and leads to

$$y_{max} \leq B\left(\frac{1}{1+C}\right)\left(\frac{C}{C+D}\right)$$

$$\simeq \frac{B}{1+C} \qquad \text{for } C \gg D \quad . \tag{4}$$

Since B is the value that would be achieved in the absence of atom quenching, we see that the yield is reduced by the ratio $1 + k_Q/2k_{R_T} \cdot M$. The approximation holds, since we will find $C \gg D$ for all the cases we consider. The second approximation solution follows directly from equation (3) by neglecting the term $D/(1-x)^2$. Then

$$y_{max} = \frac{B}{C-1}\left|\left(\frac{1}{C}\right)^{\frac{1}{C-1}} - \frac{1}{C}\right| \quad . \tag{5}$$

For $C \gg 1$, which is the case in our examples,

$$y_{max} \sim \frac{B}{C} \quad , \tag{6}$$

and we see that (6) and (4) essentially agree. Thus, we find that the largest excited molecule concentration that can be achieved is

$$(N_M^*)_{max} \leq (N_{A_o})(M)k_R^*/k_Q \quad , \tag{7}$$

This maximum N_M^* population occurs quite early in the recombination process; in fact, $x \sim \frac{1}{1+C}$ at the maximum. Since $C \sim 10^2$ to 10^3, very few atoms have recombined at the time of the maximum.

Results

We can use equation (7) and the shock tunnel parameters given above to estimate maximum gains for association of Br, Cl, and O. The pertinent parameters and results are listed in Table IV. In this table, $\Phi = k_R^*/k_{R_T}$, and the gain is calculated from the approximate formula

$$G = \frac{\lambda^2}{8\pi}\frac{A_{v'v''}}{\Delta\nu}\Delta N \quad . \tag{8}$$

Table IV

PARAMETERS OF SHOCK-TUNNEL ATOM ASSOCIATION REACTIONS

[$N_{A_o} = 1.5 \times 10^{18}/cm^3$, $M = 3 \times 10^{18}/cm^3$, $T = 2000^oK$, $p = 1$ atm]

Specie	k_{R_T} (cm^6/sec)	Φ [a]	k_Q [a] (cm^3/sec)	A (sec^{-1})	C	D	$(N_M^*)_{max}$ ($1/cm^3$)	Gain (cm^{-1})
Br	5×10^{-32} [b]	$\frac{1}{20}$ [b]	5×10^{-11} [b]	5×10^{2} [d]	1.7×10^{2}	2×10^{-4}	$\sim 5\times10^{14}$	$\leq 10^{-6}$
Cl	5×10^{-33} [b]	$\frac{1}{100}$ [b]	7×10^{-11} [b]	1.7×10^{3} [d]	2×10^{3}	2×10^{-2}	$\sim 7\times10^{12}$	$\leq 7\times10^{-8}$
O	2×10^{-33} [e]	$\frac{1}{25}$ [f]	10^{-12} [c]	~ 2 [g]	30	3×10^{-5}	$\sim 3\times10^{14}$	$\leq 2\times10^{-9}$

[a] Values at $T \sim 300^oK$. No correction for temperature is made.

[b] R. J. Browne and E. A. Ogryzlo, J. Chem. Phys. 52, 5774 (1970).

[c] T. G. Slanger and G. Black (to be published)

[d] J. A. Coxon, in Molecular Spectroscopy I, R. F. Barrow, D. A. Long, and D. J. Miller, Eds. (The Chemical Society, London, 1973).

[e] K. Schofield, Planet. Space Sci. 15, 643 (1967).

[f] Assumes statistical recombination into $O_2(A^3\Sigma_u^+)$.

[g] V. Hasson, R. W. Nicholls, and V. Dejen, J. Phys. B 3, 1192 (1970).

We assume $A_{v',v''} \sim \frac{1}{2} A$ (i.e., largest Franck-Condon factor $\sim \frac{1}{2}$), a linewidth $\Delta\nu \sim 10^{10}$ Hz, and $\Delta N \sim 10^{-3} (N_M^*)_{max}$, where the 10^{-3} accounts for vibrational and rotational distribution factors.

The assumptions made in calculating the gains of Table IV must be regarded as optimistic for three reasons:

(1) The recombination is assumed to start instantaneously with the maximum number of atoms.

(2) The lower state of the transition is assumed to be empty.

(3) The yields into excited states are assumed to be independent of temperature.

The last assumption is particularly questionable, since the excited molecular states considered have dissociation energies of $\sim$ 2000 to $\sim$ 6000 cm^{-1}. Therefore, the equilibrium for these states will be shifted almost totally toward dissociation at $T \sim 2000^{o}K$.

In spite of the favorable assumptions, the gains shown in Table IV are exceedingly small. This is due in large part to the deleterious effects of quenching by atoms, which reduces the yield of excited molecular states by factors of 30 to 2000. In addition, the transitions listed are all forbidden, and the low transition probabilities contribute to the small gains. Of course, parameters such as pressure, temperature, and mixture can be varied in the shock tunnel, but it is not expected that the results will be significantly different from those shown. These predictions are fully consistent with the experimental failure to observe gain in these systems in other laboratories.

In the case of O_2, the quenching reaction

$$O_2(A^3\Sigma_u^+) + O(^3P) \rightarrow O_2 + O(^1S)$$

leads to excited atoms with an estimated 50% efficiency.[21] Since $O(^1S)$ is the precursor to the XeO^* laser in e-beam pumped systems,[20] we can consider the possibility of a gas dynamic XeO^* laser. The sequence of reactions is

$$O + O + M \xrightarrow{k_R} O_2^* + M$$

$$O + O_2^* \xrightarrow{k_Q} O(^1S) + O_2$$

$$O + O(^1S) \xrightarrow{k_Q'} 2O(^1D)$$

$$O(^1S) + Xe + M \rightleftharpoons XeO^* + M$$

$$XeO^* \rightarrow XeO + h\nu$$

where we must now consider the additional quenching of $O(^1S)$ by $O(^3P)$. Neglecting the interactions with Xe for a moment, we find that

$$[O(^1S)]_{max} \simeq \frac{k_Q}{k_Q'} (O_2^*)_{max} \quad .$$

For $k_Q \sim 10^{-12}$ and $k_Q' \sim 10^{-11}$ cm^3/sec,[21] and for the value of $(O_2^*)_{max}$ from Table IV, we find $[O(^1S)]_{max} < 10^{13}/cm^3$. Now the recombination with Xe is very rapid, so that $O(^1S)$ and XeO^* may be considered to be in equilibrium.[22] However, the XeO^* bond strength is very weak (~ 450 cm^{-1}), so that we can estimate $XeO^*/O^* \leq 5 \times 10^{-4}$ at T = 2000°K. Thus $(XeO^*)_{max} \sim 5 \times 10^9/cm^3$ and $G \sim 10^{-7}/cm^3$ even though the transition in this case is fully allowed, with $A \simeq 4 \times 10^6$/sec.[22]

It is apparent from the above discussion that the high temperatures existing even in the expansion nozzle are detrimental to recombinations into excited states. We can consider expanding the gas to lower temperatures and pressures, but if we reduce the temperature by another factor of five (say, T ~ 400°K), the density is reduced by a factor of 60, and since molecular formation is proportional to the square of density, the trade-off is not entirely favorable.

Conclusions

We find that there are two serious handicaps to achievement of atom association lasers in the shock-tunnel environment. The first is that, for the systems studied, the combining atoms quench the newly formed excited molecules with near gas kinetic efficiency. The second is that the high temperatures of the medium reduce the recombination rate and, in fact, may shift the equilibrium toward total dissociation for the weakly bound excited molecules.

CONCLUSIONS

Our experimental efforts during this period have consisted of two "diagnostic" studies, both involving the Ba + N_2O reaction, and two studies that consider new approaches to making visible chemical lasers. In addition, we have analyzed the feasibility of a third approach to chemical lasers. In each study, the results are somewhat discouraging. The new laser approaches do not appear promising, at least from results obtained to date, and the diagnostic studies challenge our understanding of the reaction mechanisms leading to chemiluminescence. There is still a great deal of work to be done before those mechanisms are unravelled. In the meantime, achievement of a visible chemical laser will be fortuitous.

REFERENCES

1. D. J. Eckstrom, S. A. Edelstein, D. L. Huestis, B. E. Perry, and S. W. Benson, Semiannual Technical Report No. 1, Contract DAAH01-74-C-0524 (August 1974).
2. E. N. Antonov, V. G. Koloshnikov, and V. R. Mironenko, Optics Comm. 15, 99 (1975), and references therein.
3. M. A. Revelli, B. G. Wicke, and D. O. Harris, Chem. Phys. Letters (to be published).
4. K. U. Baron and B. Stadler, J. Quant. Elect. QE-11, 852 (1975).
5. D. J. Eckstrom, S. A. Edelstein, D. L. Huestis, B. E. Perry, and S. W. Benson, Semiannual Technical Report No. 3, Contract DAAH01-74-C-0524 (September 1975).
6. C. V. Shank and M. B. Klein, Appl. Phys. Letters 23, 156 (1973).
7. J. P. Reilly and G. Pimental (to be published).
8. W. Felder, R. K. Gould, and A. Fontijn, AeroChem TP-325 (July 1975).
9. R. W. B. Pearse and A. G. Gaydon, The Identification of Molecular Spectra (Chapman and Hall Ltd., London, 1963).
10. G. Black, M. Luria, D. J. Eckstrom, S. A. Edelstein, and S. W. Benson, J. Chem. Phys. 60, 3709 (1974).
11. S. E. Johnson, P. B. Scott, and G. Watson, J. Chem. Phys. 61, 2834 (1974).
12. H. A. Olschewski, J. Troe, and H. Gg. Wagner, Ber. Bensenges. Physik. Chem. 70, 450 (1966).
13. W. Felder and A. Fontijn, AeroChem TP-318 (1975).
14. B. Meyers, J. J. Smith, and K. Spitzer, J. Chem. Phys. 53, 3616 (1970).
15. R. C. Millikan and D. R. White, J. Chem. Phys. 39, 3209 (1963).
16. R. A. Young, J. Chem. Phys. 40, 1848 (1964).
17. K. E. Shuler, T. Carrington, and J. C. Light, Appl. Optics Supplement 2, 81 (1965).
18. B. Fontaine and B. Forestier, "On Potentiality of Three-Body Recombination Processes for High power Continuous Wave Visible Laser Generation,"

paper presented at 2nd National Symposium on Gas Laser Physics, Novosibirsk, June 1975; B. Forestier, B. Fontaine, and J. Valensi, "Experimental Investigation on Recombination Molecular Gas Dynamic Lasers Using the Excitation of Electronic Levels," Procedings of 10th International Shock Tube Symposium, July 1975 (to be published).

19. A. S. Biryukov, et al., JETP 40, 1025 (1975); A. Y. Volkov, et al., "Recombinational Gas Dynamic Visible O_2-Laser: Experimental and Theoretical Feasibility Study," 2nd Summer Colloquium on Electronic Transition Lasers, Woods Hole, Massachusetts, September 1975.

20. H. T. Powell, J. R. Murray, and C. K. Rhodes, Appl. Phys. Letters 25, 730 (1974).

21. T. G. Slanger and G. Black (to be published).

22. G. Black, R. L. Sharpless, and T. G. Slanger, J. Chem. Phys. 63, 4546 (1975).

HP/EGL PROGRAM REPORTS DISTRIBUTION LIST "B" - TECHNICAL REPORT

Defense Advanced Research Projects Agency, Arlington, Va.
Attn: Director, Laser Division

ODDR&E, Pentagon
Attn: Ass't Director (Space and Advanced Systems)

US Arms Control and Disarmament Agency
Department of State Bldg.
Attn: Dr. Charles Henkin

U.S. Energy Research and Development Administration, Division of Military Application
Attn: Dr. Lawrence E. Killion

NASA, Code RR, FOB 10B
Washington, D.C.

NASA, Lewis Research Center
Attn: Dr. John W. Dunning, Jr.

NASA, Ames Research Center
Attn: Dr. Kenneth W. Billman

National Security Agency
Fort George G. Meade
Attn: Mr. Richard C. Foss A763
FANX III

Dept. of the Army
Office of the Deputy Chief of Staff of Research, Dev. and Acquisition
Attn: DAMA-WS
DAMA-WSM-A (LTC. B. Pellegrini)

Dept. of the Army
Office of the Deputy Chief of Staff of Operations & Plans
Attn: DAMO-RQD (LTC Mayhew)
DAMO-RQD (LTC Fox)

Ballistic Missile Defense Program Office
Arlington, Virginia
Attn: Mr. Albert J. Bast

U.S. Army Missile Command
Redstone Arsenal
Attn: AMCPM-HEL (Mr. Jennings)
AMCPM-HEL-T (Dr. Evers)
Attn: AMSMI-RNS

U.S. Army Mobility Equipment R&D Center
Ft. Belvoir
Attn: SMEFB-MW

Rock Island Arsenal
Attn: SARRI-LR, Mr. J.W. McGarvey

U.S. Army Armament Command
Rock Island
Attn: AMSAR-RDT

Ballistic Missile Defense Advanced Technology Center
Huntsville, Alabama
Attn: ATC-O, Mr. W. O. Davies

USA Test & Evaluation Command
Aberdeen Proving Ground
Attn: AMSTE-ME (Dr. N. Pentz)

US Army Materiel Command
Alexandria, Virginia
Attn: AMCRD-T (Mr. Paul Chernoff, Dr. David Stefanye, Dr. B. Zarwyn)

US Army Ballistic Research Lab
Aberdeen Providing Ground
Attn: Dr. Robert Eichelberger, Mr. Frank Allen, Dr. E. C. Alcarez

US Army Air Defense School
Ft. Bliss, Texas
Attn: Air Defense Agency

US Army Air Defense School
Ft. Bliss, Texas
Attn: ATSA-CD-MS

US Army Training and Doctrine Command
Ft. Monroe, Virginia
Attn: ATCD-CF

USA Frankford Arsenal
Philadelphia, Pa.
Attn: Mr. M. Elnick (SARFA-FCD)

US Army Electronics Command
Ft. Monmouth, N.J.
Attn: AMSEL-CT-L (Dr. R. G. Buser)

US Army Combined Arms Combat
Developments Activity
Ft. Leavenworth, Kansas

Deputy Commandant for Combat &
Training Developments
US Army Ordnance Center and School
Aberdeen Proving Ground
Attn: ATSL-CTD-MS-R (Dr. Welch)

Dept. of the Navy
Office of the Chief of Naval Ops.
Attn: CDR L. E. Pellock
Mr. L. E. Triggs

Office of Naval Research
Boston, Mass.
Attn: Dr. Fred Quelle

Office of Naval Research
Arlington, Virginia
Attn: Dr. W. J. Condell

Dept. of the Navy
Deputy Chief of Naval Materiel (Dev)
Washington, D.C.
Attn: Mr. R. Gaylord

Naval Missile Center
Point Mugu, California
Attn: Gary Gibbs (Code 5352)

Commander, Naval Sea Systems Command
Washington, D.C.
Attn: Capt. J. G. Wilson

Naval Postgraduate School
Monterey, California
Attn: Library

U.S. Naval Weapons Center
China Lake, California
Attn: Mr. E. B. Niccum

Naval Research Lab
Washington, D.C.
Attn: Dr. J. M. MacCallum,
Dr. P. Livingston, Dr. D. J.
McLaughlin, Dr. J. L. Walsh,
Dr. J. T. Schriempf, Dr. R. F.
Wenzel, Mr. R. W. Rice,
Dr. L. R. Hettche, Dr. J. K.
Hancock

Naval Surface Weapons Center
Silver Spring, Md.
Attn: Dr. E. L. Harris, Dr. L. H.
Schindel, Mr. D. L. Merritt,
Mr. J. Wack

Hq. AFSC/XRLW
Andrews AFB
Attn: Major James M. Walton

Hq. USAF(RDPS)
Washington
Attn: LTC A. J. Chiota

Hq. AFSC(DLCAW)
Andrews AFB
Attn: Maj. H. Axelrod

Air Force Weapons Lab
Kirtland AFB, N.M.
Attn: Col. Donald L. Lamberson
Col. John C. Scholtz
Col. Russell K. Parsons
LTC John C. Rich

Hq. SAMSO
Los Angeles, California
Attn: Capt. Dorian A. DeMaio
Capt. Thomas J. Ernst

AF Avionics Lab
Wright Patterson AFB
Attn: Mr. K. Hutchinson

AF Materials Lab
Wright Patterson AFB
Attn: Maj. Paul Elder
Dr. William Frederick

Hq. Foreign Technology Division
Wright Patterson AFB
Attn: Mr. R. W. Buxton

AF Aero Propulsion Laboratory
Wright Patterson AFB
Attn: Maj. George Uhlig

RADC (OCSE/Mr. R. Urtz)
Griffiss AFB, New York

Hq. Electronics Systems Div (ESD)
Hanscom AFB
Attn: Capt. Allen R. Tobin

AF Rocket Propulsion Lab
Edwards AFB
Attn: B. R. Bornhorst

CINCSAC/INEP
Offutt AFB

USAF/INAKA
Washington, D.C.
Attn: LTC Fredric C. Dunlap

Defense Intelligence Agency
Washington, D.C.
Attn: Mr. Seymour Berler

Central Intelligence Agency
Washington, D.C.
Attn: Mr. Julian C. Nall
Dr. John E. Ashman

Aerodyne Res.
Burlington, Mass.
Attn: Charles E. Kolb

Analytic Services, Inc.
Falls Church, Virginia
Attn: Dr. John Davis

Aerospace Corp.
Los Angeles, California
Attn: Dr. G. P. Millburn
Dr. Walter R. Warren, Jr.
Dr. Elliott L. Katz

Mr. A. Colin Stancliffe
AiResearch Manuf.
Torrance, California

Atlantic Research Corp.
Alexandria, Virginia
Attn: Mr. Robert Naismith

AVCO-Everett Research Lab.
Everett, Mass.
Attn: Dr. George Sutton
Dr. Jack Dougherty

Battelle Columbus Laboratories
Columbus, Ohio
Attn: Mr. Fred Tietzel

Bell Aerospace Co.
Buffalo, N.Y.
Attn: Dr. Wayne Solomon

Boeing Co.
Seattle, Washington
Attn: Mr. M. I. Gamble

ESL Inc.
Sunnyvale, California
Attn: Mr. Harold A. Malliot

Electro-Optical Systems
Pasadena, California
Attn: Dr. Andrew Jensen

General Electric Co.
Philadelphia, Pa.
Attn: Mr. W. J. East
Dr. C. E. Anderson
Dr. R. R. Sigismonti

General Electric Co.
Pittsfield, Mass.
Attn: Mr. D. G. Harrington

General Research Corp.
Santa Barbara, California
Attn: Dr. R. Holbrook

General Research Corp.
Arlington, Virginia
Attn: Dr. Giles F. Crimi

Hercules Inc.
Wilmington, Del.
Attn: Dr. R. S. Voris

Hercules, Inc.
Cumberland, Md.
Attn: Dr. Ralph F. Preckel

Hughes Research Labs.
Malibu, California
Attn: Dr. D. Forster
Dr. Arthur N. Chester
Dr. Viktor Evtuhov
Dr. Gerald S. Picus

Hughes Aircraft Co.
Culver City, California
Attn: Dr. Eugene Peressini
Dr. John Fitts
Dr. J. A. Alcalay

Hughes Aircraft Co.
Fullerton, California
Attn: Dr. William Yates

Institute for Defense Analyses
Arlington, Virginia
Attn: Dr. Alvin Schnitzler

Johns Hopkins University
Silver Spring, Md.
Attn: Dr. Albert M. Stone
Dr. R. E. Gorozdos

Lawrence Livermore Laboratory
Livermore, California
Attn: Dr. R. E. Kidder,
Dr. E. Teller, Dr. Joe Fleck,
Dr. John Emmitt, Mr. Carl
Haussmann

Los Alamos Scientific Labs
Los Alamos, N.M.
Attn: Dr. Keith Boyer
Dr. O. P. Judd

Lulejian and Associates, Inc.
Torrance, California

Lockheed Palo Alto Research Lab.
Palo Alto, California
Attn: L. R. Lunsford

Mathematical Sciences Northwest
Bellevue, Washington
Attn: Mr. Peter H. Rose &
Mr. Abraham Hertzberg

Martin Marietta Aerospace
Denver, Colorado
Attn: Mr. Roy J. Heyman
Dr. Scott Gilles

Massachusetts Institute of Technology
Lexington, Mass.
Attn: Dr. S. Edelberg, Dr. L. C.
Marquet, Dr. J. Freedman,
Dr. G. P. Dinneen, Dr. R. H.
Rediker

McDonnell Douglas Astronautics Co.
Huntington Beach, California
Attn: Mr. P. L. Klevatt

McDonnell Douglas Research Labs
St. Louis, Mo.
Attn: Dr. D. P. Ames

MITRE Corp.
Bedford, Mass.
Attn: Mr. A. C. Cron

Dr. Anthony N. Pirri
Physical Sciences Inc.
Wakefield, Mass.

Northrup Corporation
Hawthorne, California
Attn: Dr. Gerard Hasserjian
Dr. M. M. Mann

Pacific Sierra Research Corp.
Santa Monica, California
Attn: Dr. R. Lutomirski

Philco Ford
Newport Beach, California
Attn: W. H. Rohrer

RAND Corp.
Santa Monica, California
Attn: Dr. Claude R. Culp

Raytheon Co.
Waltham, Mass.
Attn: Dr. Frank A. Horrigan

Raytheon Co.
Bedford, Mass.
Attn: Dr. H. A. Mehlhorn

Raytheon Co.
Waltham, Mass.
Attn: Dr. Hermann Statz

RCA
Morrestown, N.J.
Attn: Mr. J. A. Colligan
Information Control

Riverside Research Institute
New York, N.Y.
Attn: Dr. L. H. O'Neill
Dr. John Bose
HPEGL Library

R&D Associates
Santa Monica, California
Attn: Dr. R. E. LeLevier
Dr. R. Hundley

Rockwell International Corp.
Anaheim, California
Attn: R. E. Hovda
Dr. J. Winocur

Rockwell International Corp.
Albuquerque, N.M.
Attn: Mr. C. K. Kraus

SANIDA Laboratories
Albuquerque, N.M.
Attn: Dr. A. Narath

W. J. Schafer Associates
Wakefield, Mass.
Attn: Francis W. French

Stanford Research Institute
Menlo Park, California
Attn: Dr. R. A. Amistead
Mr. J. E. Malick

Science Applications, Inc.
La Jolla, California
Attn: Dr. John Asmus

Mr. Lawrence Peckham
Science Applications Inc.
Arlington, Virginia

Science Applications, Inc.
Ann Arbor, Michigan
Attn: Dr. R. E. Meredith

Dr. Robert Greenberg
Science Applications, Inc.
Bedford, Mass.

Systems Consultants, Inc.
Washington, D.C.
Attn: Dr. Robert B. Keller

Systems, Science and Software
La Jolla, California
Attn: Mr. Alan F. Klein

Thiokol Chemical Co.
Brigham City, Utah
Attn: Mr. James E. Hansen

TRW Systems Group
Redondo Beach, California
Attn: Mr. Norman F. Campbell

TRW Systems Group
Redondo Beach, California
Attn: Mr. Eugene M. Noneman

United Aircraft Research Lab.
East Hartford, Conn.
Attn: Mr. G. H. McLafferty
Mr. Albert Angelbeck

United Aircraft Corp.
West Palm Beach, Florida
Attn: Dr. R. A. Schmidtke
Mr. Ed Pinsley

Varian Associates
San Carlos, California
Attn: Mr. Jack Quinn

Vought Systems Division
Dallas, Texas
Attn: Mr. F. G. Simpson

Westinghouse Electric Corp.
Baltimore, Md.
Attn: Mr. W. F. List

Westinghouse Research Lab
Pittsburgh, Pa.
Attn: Dr. E. P. Riedel
Mr. R. L. Hundstad